ACS Medicinal Chemistry Letters

UNIVERSITY OF EXETER

Subscriber access provided by the University of Exeter

Letter

Synthesis, Biological Evaluation and Molecular Docking of Arylpyridines as Anti-proliferative Agent Targeting Tubulin

JiaPeng He, Mao Zhang, Lv Tang, Jie liu, JiaHong Zhong, Wenya Wang, Jiang-Ping Xu, Hai-Tao Wang, Xiao-Fang Li, and Zhong-Zhen Zhou

ACS Med. Chem. Lett., **Just Accepted Manuscript** • DOI: 10.1021/acsmedchemlett.0c00278 • Publication Date (Web): 15 Jul 2020

Synthesis, Biological Evaluation and Molecular Docking of Arylpyridines as Anti-proliferative Agent Targeting Tubulin

JiaPeng He,[†, #] Mao Zhang,[†, #] Lv Tang,[†, #] Jie liu,[†] JiaHong Zhong,[†] Wenya Wang,[†] Jiang-Ping Xu,[†, ‡] Hai-Tao Wang,[†] Xiao-Fang Li [§] and Zhong-Zhen Zhou*[, †]

[†]Innovation Program of Drug Research on Neurological and Metabolic Diseases, Guangdong Provincial Key Laboratory of New Drug Screening, School of Pharmaceutical Sciences, Southern Medical University, Guangzhou, 510515, China

[‡] Key Laboratory of Mental Health of the Ministry Education, Southern Medical University, Guangzhou 510515, China

[§] Department of Hematology, Nanfang Hospital, Southern Medical University, Guangzhou 510515, China.

ABSTRACT: Mimicking different pharmacophoric units into one scaffold is a promising structural modification tool to design new drugs with enhanced biological properties. To continue our research on the tubulin inhibitors, the synthesis and biological evaluation of arylpyridine derivatives (**9-29**) are described herein. Among these compounds, 6-arylpyridines (**13-23**) bearing benzo[d]imidazole side chains at 2-position of pyridine ring displayed selective antiproliferative activities against HT-29 cells. More interestingly, 2-trimethoxyphenylpyridines **25**, **27,** and **29** bearing benzo[d]imidazole and benzo[d]oxazole side chains displayed more broad-spectrum antitumor activities against all tested cancer cell lines. **29** bearing 6-methoxybenzo[d]oxazole group exhibited comparable activities against A549 and U251 cells to combretastatin A-4 (CA-4), and lower cytotoxicities than CA-4 and 5-Fu. Further investigations revealed **29** display strong tubulin polymerization inhibitory activity (IC_{50} = 2.1 μM), and effectively bind at the colchicine binding site, and arrest the cell cycle of A549 in the G2/M phase by disrupting microtubules network.

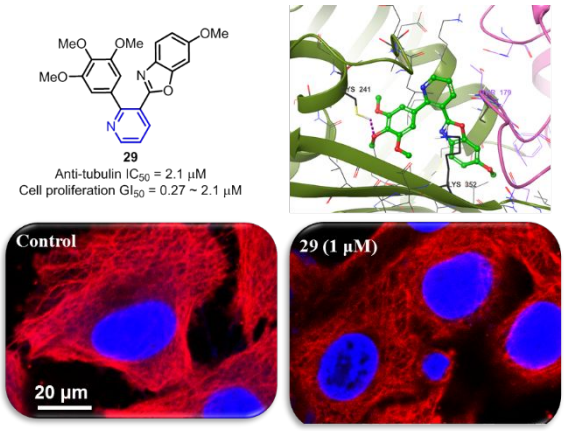

KEYWORDS: arylpyridines, antiproliferative activities, tubulin polymerization inhibitor, cell cycle arrest, molecular docking

It is widely known that malignant tumors always compromise human health [1]. However, recovery rates of cancer patients have improved in recent years with the emergence of new antitumor drugs. It is commonly known that microtubules, an effective target for cancer chemotherapy, play important roles in various cellular functions, and participate in the formation of mitotic bipolar spindles [2-3]. By altering microtubule dynamics at the mitotic stage, microtubule-targeting agents (MTAs), also called antimitotic drugs, directly interrupt spindle microtubules and arrest cells in the G2/M phase. Microtubules contain six unique binding sites (taxanes, vinca alkaloids, epothilone, laulimalide, pironetin, and colchicine domains)[4-5]. And the epothilone binding site is an undistinct site, which has been proposed in the taxane pocket of β-tubulin[6]. Currently, several MTAs are approved for the treatment of tumors, and these include paclitaxel [7-8], vinca alkaloids[9], eribulin (vinca binding site inhibitors)[10], and ixabepilone (taxanes binding site inhibitor) [11].

However, none of the approved tubulin inhibitors target the colchicine domain for treating the tumor. Despite all this, extensive efforts have been made to promote the discovery of colchicine site inhibitors[12-13]. The cis-stilbene combretastatin A-4 (CA-4, Fig. 1) is one of the most anti-tubulin active compounds by strongly binding to the colchicine site in β-tubulin[14]. The cis-configuration of the double bond connecting two ring moieties present in the structures is very important for the high cytotoxic and anti-tubulin activities of combretastatin derivatives. To avoid the cis-trans isomerization, many efforts have focused on the replacement of the double bond with a ring or other functionalities to increase the biological efficiency and minimize possible metabolism[14-15]. Interestingly, numerous novel microtubule-destabilizing agents with six-membered heterocyclic bridging groups displayed potential activities. Among them, sulfonamide tubulin polymerization inhibitor (ABT-751, Figure 1) [16] with a pyridine bridging group is reported to cause a significant reduction in rat tumor blood flow and was well tolerated in the clinical trial [17-18]. Pyridine-bridged analogs (3) with a 3-atom distance between two phenyl rings exhibited comparable antitumor activity to CA-4 and blocked angiogenesis in *vivo*[19].

Our recent research were mainly focused on potential heterocyclic anticancer agents based on different kinds of heterocyclic scaffolds.[20-22] Our reported compounds 4 and 5 with purine bridging group displayed promising antitumor activities and lower cytotoxicity in normal cells, but weak tubulin polymerization inhibition activity [20]. Nevertheless, the potent biological profile encouraged us to continue our search

for high-potency antitumor drugs. Herein, different skeleton modifications on the CA-4 scaffold were described, especially the replacement of the olefinic bond with pyridine ring and the incorporation of five-membered heterocyclic rings (such as benzo[d]imidazoles, benzo[d]thiazoles and benzo[d]oxazoles). Many tubulin polymerization inhibitors with these five-membered heterocyclic rings displayed strong activities [23-27], such as compounds **6** [27], **7** [26], and **8**[25]. Consequently, arylpyridines (**9-29**, Figure 1) with benzo[d]imidazole, benzo[d]thiazole and benzo[d]oxazole side chains were designed and synthesized in the current study. The antiproliferative activities, arresting the cell cycle abilities, and tubulin polymerization inhibitory activities of these obtained derivatives were subsequently evaluated. To better understand structure-activity relationships, molecular docking was also performed.

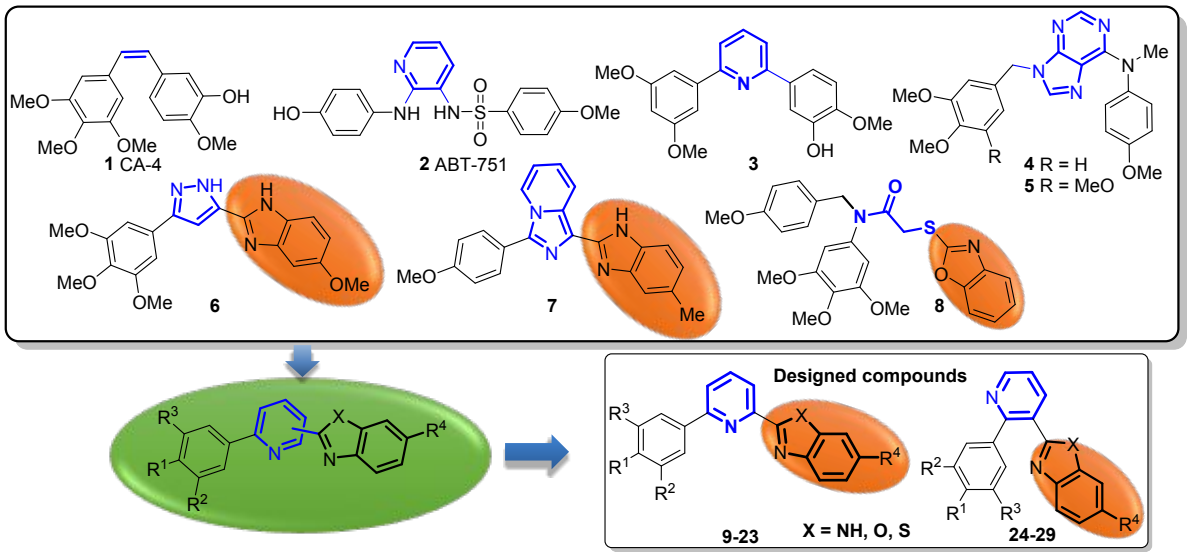

Figure 1. Examples of some reported tubulin polymerization inhibitors and the proposed design of novel arylpyridine conjugates (**9-29**) containing benzo[d]imidazole, benzo[d]thiazole and benzo[d]oxazole side chains.

Scheme 1. Synthetic routes for arylpyridines 9-29.

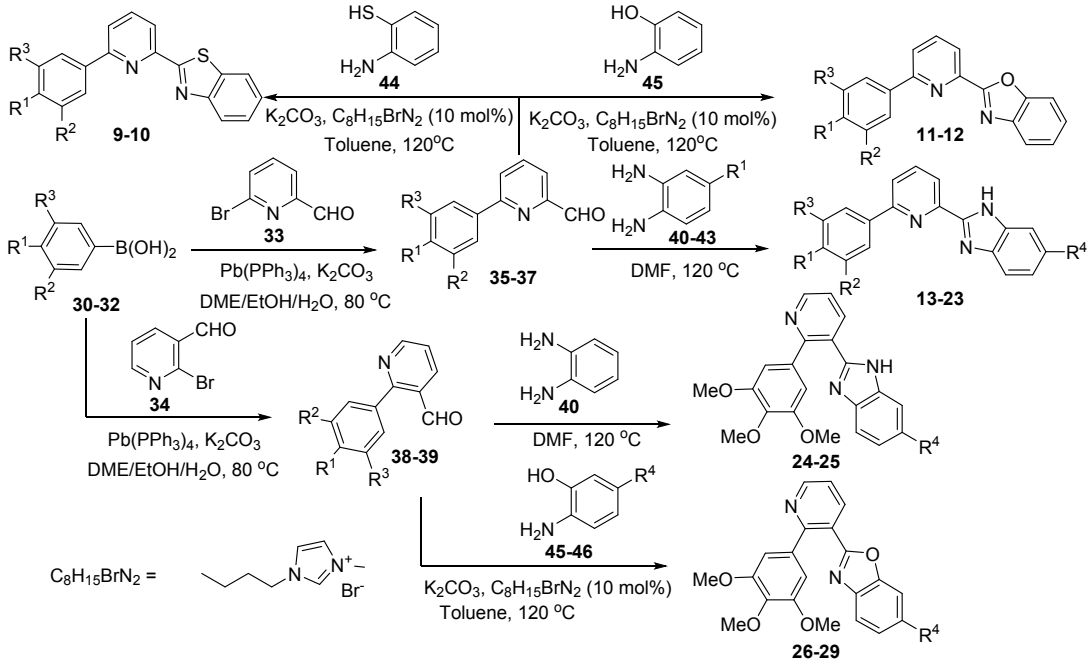

The synthetic routes of the arylpyridines (**9-29**) are illustrated in Scheme 1. Overall, the arylpyridylaldehyde (**35-39**) intermediates were prepared by the Suzuki reaction of bromopicolinaldehydes (**33-34**) with the substituted phenylboronic acid (**30-32**). Arylpyridines bearing benzo[d]thiazole side chains (**9-10**) and benzo[d]oxazole side chains (**11-12** and **26-29**) were prepared by one-pot aerobic oxidative condensation of arylpyridylaldehydes (**35-39**) with substituted 2-aminophenols and 2-aminobenzenethiol respectively, using 1-butyl-3-methylimidazolium bromide as the catalyst. 6-arylpyridines (**13-25**) possessing the benzo[d]imidazole side chains were synthesized by the

heterocyclic condensation of arylpyridylaldehydes with substituted o-phenylenediamines.

Table 1. Antiproliferative activity of arylpyridine derivatives 9-29

No.	Structure	GI_{50} (μM) [a]			Polymerization [% (10 μM), IC_{50} (μM)][b]	CC_{50} (μM) [c]
		HT-29	A549	U251		HT22
9	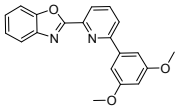	> 20	> 20	> 20	96 ± 1	- [d]
10	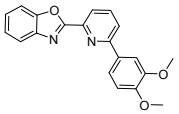	> 20	> 20	> 20	89 ± 2	- [d]
11	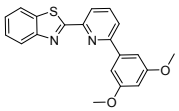	> 20	> 20	> 20	77 ± 2	- [d]
12	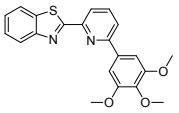	> 20	> 20	> 20	81 ± 7	- [d]
13	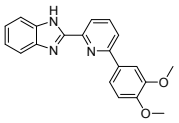	1.4 ± 0.3	> 10	> 10	78 ± 5	17.1 ± 1.2
14	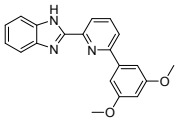	5.1 ± 0.1	> 10	> 10	80 ± 8	- [d]
15	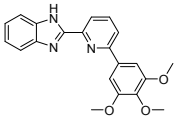	1.1 ± 0.1	> 10	> 10	90 ± 3	16.0 ± 2.7
16	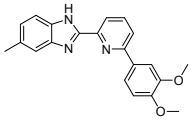	5.4 ± 0.2	> 10	> 10	87 ± 4	- [d]
17	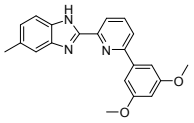	5.9 ± 0.2	> 10	> 10	74 ± 6	- [d]
18	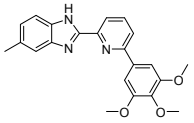	4.6 ± 0.2	> 10	7.9 ± 1.5	82 ± 5	- [d]
19	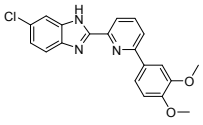	6.0 ± 1.2	> 10	> 10	96 ± 2	- [d]

No.	Structure	GI_{50} (μM) [a]			Polymerization [% (10 μM), IC_{50} (μM)][b]	CC_{50} (μM) [c]
		HT-29	A549	U251		HT22
20	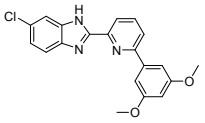	1.2 ± 0.3	> 10	> 10	69 ± 4	19.0 ± 1.5
21	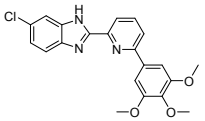	9.6 ± 0.6	8.8 ± 0.2	> 10	85 ± 1	- [d]
22	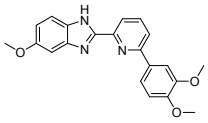	0.96 ± 0.08	> 10	> 10	86 ± 3	20.5 ± 2.1
23	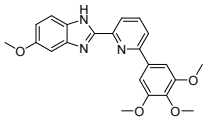	7.9 ± 0.1	> 10	8.3 ± 0.9	85 ± 4	- [d]
24	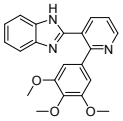	12.5 ± 1.2	> 20	> 20	81 ± 3	- [d]
25	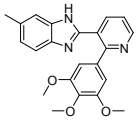	2.9 ± 0.2	2.8 ± 0.2	1.7 ± 0.2	44 ± 2 (11.7 ± 0.5)	2.7 ± 0.4
26	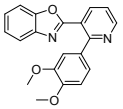	> 20	> 20	> 20	84 ± 2	- [d]
27	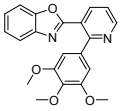	5.2 ± 0.5	7.9 ± 1.1	4.6 ± 0.6	58 ± 4	25.6 ± 0.6
28	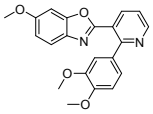	> 20	> 20	> 20	89 ± 3	- [d]
29	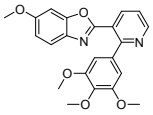	2.1 ± 0.1	0.89 ± 0.1	0.27 ± 0.04	6 ± 2 (2.1 ± 0.2)	24.8 ± 0.7
DMSO		\	\	\	100	\
CA-4	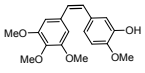	0.20 ± 0.06	0.82 ± 0.02	0.17 ± 0.02	5 ± 2 (1.6 ± 0.1)	13.9 ± 1.7
5-Fu		12.6 ± 1.6	10.7 ± 2.6	30.1 ± 2.9	\	8.1 ± 0.2

[a] GI_{50} is the dose for 50% cells growth inhibition after 48h of incubation. The GI_{50} values (means ± SDs) were averaged over at least two independent experiments ; [b] Tubulin polymerization assay conditions *in vitro*: tested compounds (10 μM), and tubulin (4 mg/mL), 40 min, 37 °C; DMSO (0.1% v/v) was used as blank (100%: no inhibition). [c] CC_{50} values represent the 50% cytotoxic concentration after 48h. All data were averaged over three separate experiments. All data were averaged over three separate experiments; [d] Not tested.

Antiproliferative activities (GI_{50}) of arylpyridines (**9-29)** were evaluated against three human cancer cell lines [HT-29 (Human colon carcinoma), A549 (Human non-small cell lung cancer cells), and U251 (glioma)], using fluorouracil (5-Fu) and CA-4 as the reference cytotoxic compounds. The growth inhibitory concentration values (GI_{50}) against tumor cells indicate 50% growth inhibition of cell growth compared to untreated controls after 48 h of incubation (Table 1).

As shown in Table 1, 6-arylpyridines bearing benzo[*d*]thiazole side chains (**9-10)** and benzo[*d*]oxazole side chains (**11-12)** at the 2-position of the pyridine ring displayed noninhibitory activities toward tested cancer cell lines. However, 2-arylpyridines bearing benzo[*d*]oxazole side chains (**27** and **29)** at the 3-position of the pyridine ring showed satisfactory activities toward all tested cancer cell lines and higher activities than 5-Fu. Intriguingly, the activities of compound **29** against the A549 and U251 cell lines reached sub-micromole values (GI_{50} = 0.89 and 0.17 μM respectively), which were comparable to that of the positive control CA-4. Besides, the toxicity evaluation in mouse normal hippocampal neurons (HT22) cells demonstrated that **27** and **29** exhibited lower cytotoxicities than the positive control CA-4.

For arylpyridines (**13-25**) bearing benzo[*d*]imidazole side chains, most of them exhibited very weak antiproliferative activities against A549 and U251 cell lines, but highly antiproliferative activities against HT-29 cells than 5-Fu (GI_{50} = 12.6 μM). Among these compounds, compounds **13, 15**, **20,** and **22** displayed more potential activities (0.96 < GI_{50} < 1.4 μM) against HT-29 cells, and lower cytotoxicity in normal HT22 cells than CA-4 and 5-Fu. Compound **25** bearing 5-methyl benzo[*d*]imidazole side chains at 3-position of pyridine ring showed good activities against HT29 (GI_{50} = 2.9 μM), A549 (GI_{50} = 2.8 μM), and U251 (GI_{50} = 1.7 μM) cell lines, but higher cytotoxicities in normal HT22 cells than the positive control CA-4 and 5-Fu.

Further structure-activity relationship results indicated that the number of methoxy groups on the benzene ring and suitable position of side chains (benzo[*d*]imidazole, benzo[*d*]thiazole and benzo[d]oxazole) in pyridine ring are essential for their selectivity and antiproliferative activities. Firstly, dimethoxyphenylpyridines bearing benzo[*d*]imidazole side chains showed selective antiproliferative activities against HT-29 cells, such as compounds **13**, **14**, **16**, **17**, **19**, **20,** and **22.**

Secondly, trimethoxyphenylpyridines bearing substituted benzo[*d*]imidazole displayed more broad-spectrum antitumor activities. For example, trimethoxyphenylpyridines **15** and **24** bearing non-substituted benzo[*d*]imidazole selectively inhibited HT-29 cells. However, trimethoxyphenylpyridines **18, 21** and **25** bearing substituted benzo[*d*]imidazole displayed good antitumor activity toward A549 cells or U251 cells. Trimethoxyphenylpyridines **25** bearing 5-methyl benzo[*d*]imidazole side chains at 3-position of pyridine ring displayed broad-spectrum antitumor activities toward tested tumor cells.

Thirdly, 2-trimethoxyphenylpyridines (such as **27** and **29**) displayed higher activities than 2-dimethoxyphenylpyridines (such as **26** and **28**). As reported in the literature, trimethoxyphenyl (TMP) moiety of combretastain A-4 analogues (tubulin colchicine binding site inhibitors) is an important pharmacophore for interaction with tubulin[15, 28]. The replacement of trimethoxyphenyl group with 3,4-dimethoxyphenyl group can lead to a decrease in activity[19, 24]. The possible reason is that replacing trimethoxyphenyl group with 3,4-dimethoxyphenyl group will cause the hydrogen bond with tubulin to weaken. Furthermore, benzo[*d*]oxazole side chains at 3-position of pyridine ring are favorable for antiproliferative activities. 2-trimethoxyphenylpyridines **27** and **29** bearing 3-benzo[*d*]oxazole side chains displayed satisfactory activities against all tested tumor cells, which were higher than that of 5-Fu. Finally, introducing the methoxy group into benzo[*d*]oxazole is conducive to the improvement of the activity. The activities of compound **29** (0.89 < GI_{50} < 2.1 μM) bearing 6-methoxybenzo[*d*]oxazole group was higher than that of **27** (4.6 < GI_{50} < 7.9 μM) bearing benzo[*d*]oxazole group.

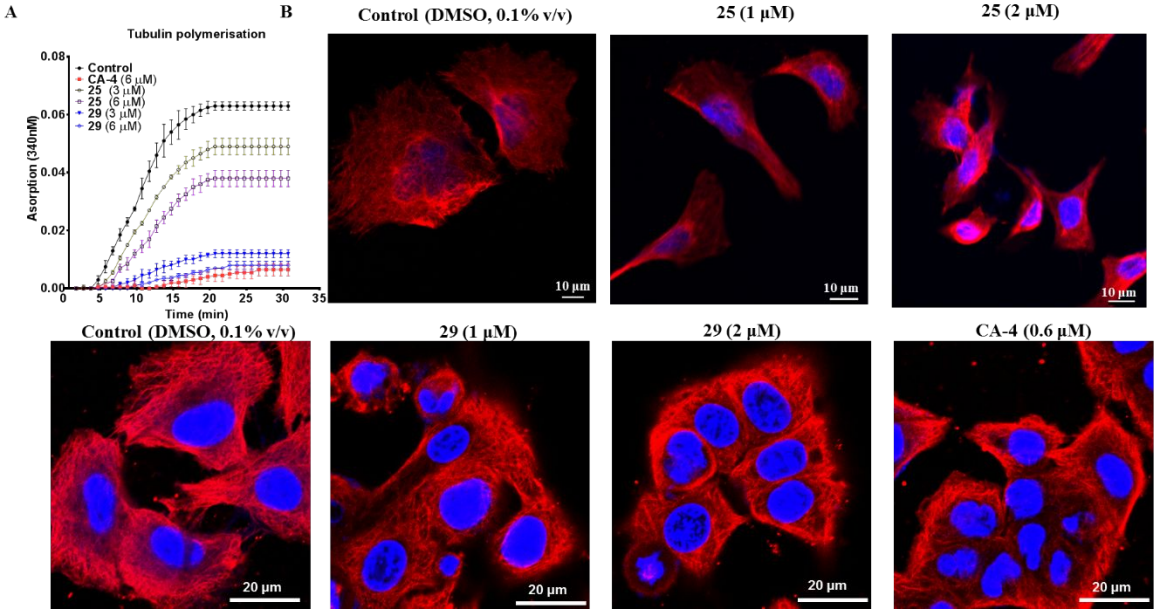

Figure 2. A) Effect of arylpyridines **25**, **29** and CA-4 on in vitro tubulin polymerization. DMSO (0.1% v/v) was used as vehicle control. B) Effect of 25 on the cellular microtubule networks of A549 cells. C) Effect of **29** on the cellular microtubule networks of A549 cells. Microtubules and DNA are stained in red and blue respectively. Untreated cells (DMSO, 0.1% v/v) were used as a negative control, and cells treated with CA-4 (0.6 μM) were used as a positive control.

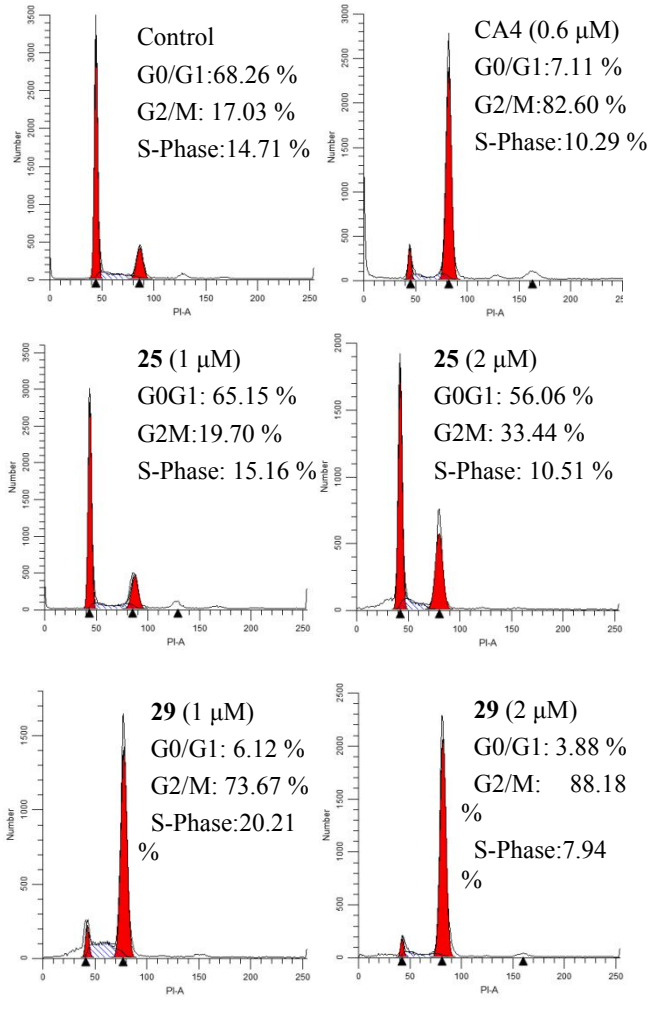

Figure 3. Analysis of the effects of **25** and **29** on the cell cycle distribution in the A549 cells using the flow cytometry analysis. DMSO (0.1% v/v) and CA-4 (0.6 μM) were utilized as a blank control and a positive control respectively. DNA content was determined by DNA intercalating dye and propidium iodide staining.

To validate the relationship between the antiproliferative activities, in vitro microtubule dynamics of arylpyridine derivatives were investigated using microtubule-destabilizing agent CA-4 as controls. Tubulin polymerization assay results indicated the tubulin polymerization inhibition ability of these compounds was increased by introducing side chains into 3-position of the pyridine ring. All arylpyridine derivatives **9-23** with side chains at 2-position of pyridine ring showed very weak activities (74% to 96% polymerization grade compared with the DMSO control). arylpyridine derivatives **24-29** with side chains at 3-position of pyridine ring displayed strong to weak polymerization inhibitory activities at a concentration of 10 μm. Among these compounds, **25** and **27** with good activities against all tested tumor cells produced good anti-tubulin polymerization activities. As shown in **Table 1** and **Figure 2A**, **29** bearing 6-methoxybenzo[d]oxazole group at the 3-position of the pyridine ring showed best polymerization inhibitory activity (IC_{50} = 2.1 μM), which was closed to that of CA-4 (IC_{50} = 1.6 μM). These results demonstrated that their antiproliferative activities may be caused by their anti-tubulin polymerization activities.

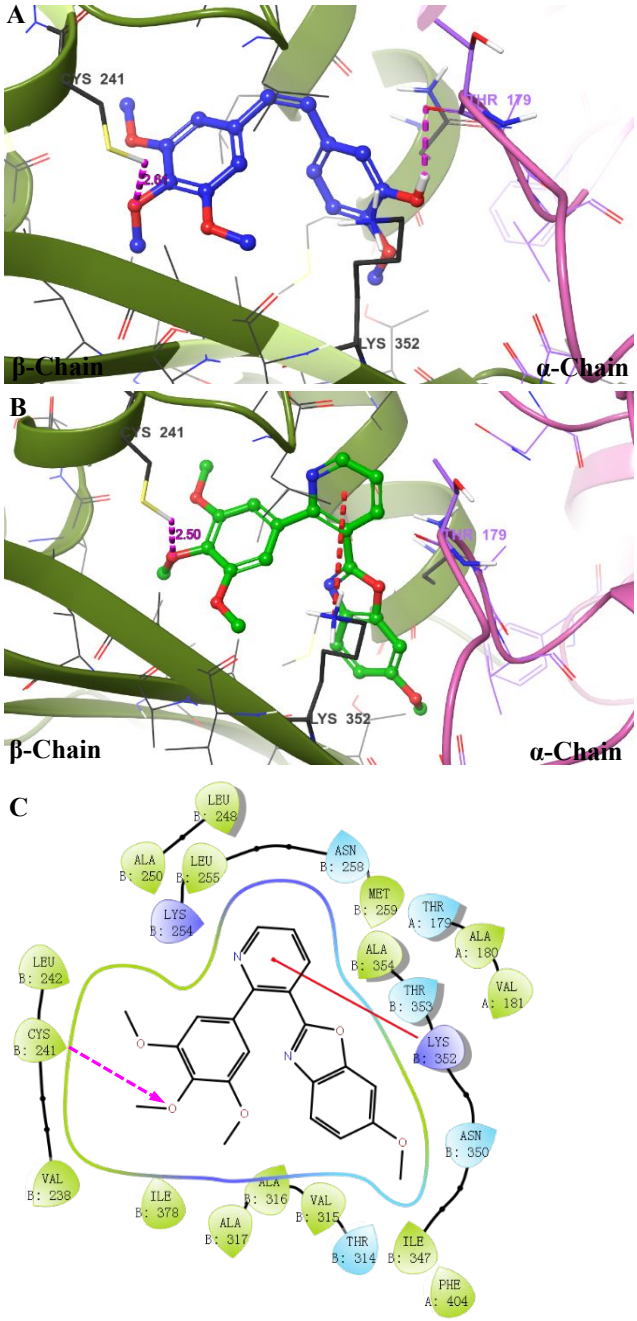

Figure 4. A) The proposed binding models of **29** (shown in green ball and stick model) with tubulin (PDB: 5LYJ). B) The native CA-4 ligand is illustrated in a blue ball and stick model. The glide docking scores of **29** and CA-4 are 8.349 and 8.864, respectively. In the 2D representation (C) of the ligand−protein interactions, all residues within 3 Å of the ligand (**29**) are shown. The intermolecular hydrogen bond is colored in magenta dash line. The π-cation interaction is colored in a red dash line (B) or a red solid line (C).

Non-small cell lung cancer (NSCLC), the main subtype of lung cancer, is the leading cause of cancer deaths worldwide. And drugs for NSCLC has been a hot and difficult problem. Thus, A549 cells were used in immunofluorescence staining assay to examine the effects of the most potent compounds **25** and **29** on the cellular microtubule networks (**Figure 2B**). After treatment with **25, 29,** and CA4 for 18h, the microtubule morphology (red) was visualized. As shown in **Figure 2B**, the

microtubule network was a normal arrangement and organization in untreated A549 cells. In contrast, the interphase microtubule network around the cell nucleus was disrupted dramatically by **25**, **29,** and **CA4**, resulting in disassembly and fragmentation. These results confirm that **25** and **29** were like CA-4 inducing tubulin depolymerization and disturbing microtubule networks.

Tubulin depolymerization and disruption of microtubule networks can induce the G2/M arrest. Thus, the arrest effects of compound **25** and **29** on the cell cycle of A549 cells was measured at different concentrations via flow cytometry after 48 h of treatment, and following propidium iodide (PI) staining of the cells (Figure 3). As illustrated in **Figure 3**, compounds **25**, **29,** and **CA-4** showed the same behavior, arrested the cell cycle of A549 cells at the G2/M phase. At the same concentration, the percentage of cells in the G2/M phase arrested by compound **29** was higher than the percentage of cells in the G2/M phase arrested by compound **25.** As the concentration of **29** increased from 0 to 2 μM, the percentage of cells in the G2/M phase was increased from 17.03% to 88.18%. Thus, compound **29** caused a significant G2/M arrest in the A549 cells in a concentration-dependent manner. The cell cycle arrest effects of **29** correlated well with its strong anti-tubulin and antiproliferative activities.

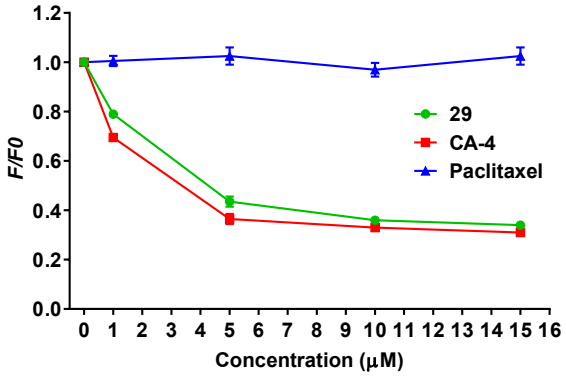

Figure 5. Based on fluorescence, colchicine competitive binding assays of compound **29** were performed in the 5.0 μM colchicine-tubulin complex at various concentrations, using CA-4 and paclitaxel positive control and negative control respectively. Percent inhibition was determined by the ratio of F/F0, whereas F0 is the fluorescence of samples without inhibitor, and F is the fluorescence of samples with inhibitor at various concentrations.

In general, CA4-like derivatives with trimethoxyphenyl groups and cis-conformation inhibits colchicine binding to tubulin.[15] To investigate the potential binding site of **29** in tubulin (PDB: 5LYJ)[28] at the colchicine site, molecular docking simulations were performed in Maestro 11.1. After the native ligand (CA-4) was re-docked into the active site cavity, the Glide RMSD (resulting root mean square deviation) value was given as 0.666 Å, which confirmed the reliability of our docking method. As shown in **Figure 4**, **29** adopted a similar conformation in the colchicine site to that of CA-4. The trimethoxyphenyl moiety of **29** formed one hydrogen bond with the β/Cys241 residue, and hydrophobic interactions with β/Cys241, β/Leu242, β/Ala250, β/Lys352, and β/Ala354. The intermolecular hydrogen bonding distance between **29** and β/Cys241 residue is 2.50Å, which is shorter than that of CA-4 with β/Cys241 residue. Moreover, the pyridine bridging group occupied the position of the double bond bridging group of CA-4, forming π-cation interaction with β/Lys352 and hydrophobic interactions with β/Asn258, β/Leu248, and α/Thr179. The 6-methoxybenzo[*d*]oxazole scaffold occupied the position of the 3-hydroxy-4-methoxyphenyl moiety of CA-4. Compared with CA-4, 6-methoxybenzo[*d*]oxazole group cannot form hydrogen bonds with surrounding amino acid residues, but it formed more hydrophobic interactions with the α/Val181, α/Val180, β/Asn258, β/Met259, β/Val315, β/Ala317, β/Ile347, β/Asn350, and β/Lys352 residues. To further confirm whether compound 29 could bind to the colchicine site on tubulin, the colchicine competitive binding assay of compound **29** was performed using CA-4 and paclitaxel as a positive control and a negative control respectively. As shown in Figure 5, the fluorescence (F) of the colchicine-tubulin complex was reduced by compound 29 in a dose-dependent manner. Combined with the results of the molecular modeling study, these indicated that the binding site of **29** is located at the colchicine binding site of tubulin.

In summary, a series of arylpyridines **9-29** containing benzo[*d*]imidazole, benzo[*d*]thiazole, and benzo[*d*]oxazole side chains was successfully designed and synthesized. Among these compounds, four 6-arylpyridines (**13, 15**, **20,** and **22)** bearing benzo[*d*]imidazole side chains at 2-position of pyridine ring showed selective antiproliferative activities against the HT-29 colon carcinoma cell line in the range of 0.96 μM to 1.4 μM. 2-Trimethoxyphenylpyridines **25, 27,** and **29** bearing benzo[*d*]imidazole and benzo[d]oxazole side chains at 3-position of pyridine ring displayed more broad-spectrum antitumor activities against all tested cancer cell lines (HT29, A549, and U251 cells). 2-Trimethoxyphenylpyridine **25** bearing 5-methyl benzo[*d*]imidazole side chains at 3-position of pyridine ring showed good activities ($1.7 < GI_{50} < 2.9$ μM) against all tested cancer cell lines (HT29, A549, and U251 cells), but higher cytotoxicities in normal HT22 cells than the positive control CA-4 and 5-Fu. However, 2-trimethoxyphenylpyridines **27** and **29** bearing the benzo[*d*]oxazole side chains with satisfactory antiproliferative activities against three different cancer cell lines displayed lower cytotoxicities in normal HT22 cells than the positive control CA-4 and 5-Fu. What's exciting is that compound **29** displayed comparable antiproliferative activities against A549 (GI_{50} = 0.82 μM) and U251 (GI_{50} = 0.17 μM) cell lines to CA-4.

Tubulin polymerization assay results indicated all 6-arylpyridine derivatives **9-23** showed very weak activities, whereas 2-arylpyridine derivatives **24-29** displayed weak to strong polymerization inhibitory activities. Among these compounds, 2-trimethoxyphenylpyridine **25** bearing benzo[*d*]imidazole side chains showed moderate tubulin polymerization inhibition activity (IC_{50} = 2.1 μM), whereas 2-trimethoxyphenylpyridines **29** bearing the benzo[*d*]oxazole side chains displayed strong tubulin polymerization inhibition activity (IC_{50} = 2.1 μM). Further investigations revealed **29** effectively bind at the colchicine binding site, and arrest the cell cycle of A549 in the G2/M phase by disrupting microtubules network. These results provide further guidance for the discovery of new CA-4 analogs with lower cytotoxicities.

ASSOCIATED CONTENT

Supporting Information

The Supporting Information is available free of charge at https://pubs.acs.org/

Experimental details (synthetic experimental details, pharmacological assays, molecular docking, and (^{1}H and ^{13}C) spectral information) are found in the supporting information of this article (PDF).

AUTHOR INFORMATION

Corresponding Author

* (Zhong-Zhen Zhou) E-mail: zhouzz@smu.edu.cn

Author Contributions

# These authors contributed equally to this work. In addition, all authors have given approval to the final version of the manuscript.

ACKNOWLEDGMENT

This work was financially supported by Foundation for Distinguished Young Teachers in Higher Education of Guangdong Province (Yue Teacher (2014)145), Natural Science Foundation of Guangdong Province (2018A030313046), and National Natural Science Foundation of China (No. 81872735).

ABBREVIATIONS

CA-4, Combretastatin-A4; NSCLC. Non-small cell lung cancer; HT22, Hippocampal neuron (HT22); HT-29, Human colon carcinoma); A549, Human non-small cell lung cancer cells; U251, glioma); 5-Fu, fluorouracil;

REFERENCES

1. Sun, Y. J.; Hu, Y. J.; Jin, D.; Li, J. W.; Yu, B., Health-related Quality of Life After Treatment for Malignant Bone Tumors: A Follow-up Study in China. *Asian Pac. J. Cancer Prev.* **2012,** *13* (7), 3099-3102.

2. Bates, D.; Eastman, A., Microtubule destabilising agents: far more than just antimitotic anticancer drugs. *Br. J. Clin. Pharmacol.* **2017,** *83* (2), 255-268.

3. Zhao, Y.; Mu, X.; Du, G., Microtubule-stabilizing agents: New drug discovery and cancer therapy. *Pharmacol. Ther.* **2016,** *162*, 134-143.

4. Liu, Y.-M.; Chen, H.-L.; Lee, H.-Y.; Liou, J.-P., Tubulin inhibitors: a patent review. *Expert Opin. Ther. Pat.* **2014,** *24* (1), 69-88.

5. Coulup, S. K.; Georg, G. I., Revisiting microtubule targeting agents: α-Tubulin and the pironetin binding site as unexplored targets for cancer therapeutics. *Bioorg. Med. Chem. Lett.* **2019,** *29* (15), 1865-1873.

6. Ranade, A. R.; Higgins, L.; Markowski, T. W.; Glaser, N.; Kashin, D.; Bai, R.; Hong, K. H.; Hamel, E.; Hofle, G.; Georg, G. I., Characterizing the Epothilone Binding Site on β-Tubulin by Photoaffinity Labeling: Identification of β-Tubulin Peptides TARGSQQY and TSRGSQQY as Targets of an Epothilone Photoprobe for Polymerized Tubulin. *J. Med. Chem.* **2016,** *59* (7), 3499-3514.

7. Weaver, B. A., How taxol/paclitaxel kills cancer cells. *Mol. Biol. Cell* **2014,** *25* (18), 2677-2681, 2675 pp.

8. Zhou, J.; Qian, S. K.; Li, H. S.; He, W. X.; Tan, X. J.; Zhang, Q.; Han, G. D.; Chen, G. Q.; Luo, R. C., Predictive value of microtubule-associated protein Tau in patients with recurrent and metastatic breast cancer treated with taxane-containing palliative chemotherapy. *Tumor Biol.* **2015,** *36* (5), 3941-3947.

9. Saez-Calvo, G.; Sharma, A.; Balaguer, F. d. A.; Barasoain, I.; Rodriguez-Salarichs, J.; Olieric, N.; Munoz-Hernandez, H.; Berbis, M. A.; Wendeborn, S.; Penalva, M. A.; Matesanz, R.; Canales, A.; Prota, A. E.; Jimenez-Barbero, J.; Andreu, J. M.; Lamberth, C.; Steinmetz, M. O.; Diaz, J. F., Triazolopyrimidines Are Microtubule-Stabilizing Agents that Bind the Vinca Inhibitor Site of Tubulin. *Cell Chem. Biol.* **2017,** *24* (6), 737-750.e736.

10. Aseyev, O.; Ribeiro, J. M.; Cardoso, F., Review on the clinical use of eribulin mesylate for the treatment of breast cancer. *Expert Opin. Pharmacother.* **2016,** *17* (4), 589-600.

11. Kaur, R.; Kaur, G.; Gill, R. K.; Soni, R.; Bariwal, J., Recent developments in tubulin polymerization inhibitors: An overview. *Eur. J. Med. Chem.* **2014,** *87*, 89-124.

12. Xia, L. Y.; Zhang, Y. L.; Yang, R.; Wang, Z. C.; Lu, Y. D.; Wang, B. Z.; Zhu, H. L., Tubulin inhibitors binding to colchicine-site: A Review from 2015 to 2019. *Curr. Med. Chem.* **2019,** *26*, 1-27.

13. Naaz, F.; Haider, M. R.; Shafi, S.; Yar, M. S., Anti-tubulin agents of natural origin: Targeting taxol, vinca, and colchicine binding domains. *Eur. J. Med. Chem.* **2019,** *171*, 310-331.

14. Bukhari, S. N. A.; Kumar, G. B.; Revankar, H. M.; Qin, H.-L., Development of combretastatins as potent tubulin polymerization inhibitors. *Bioorg. Chem.* **2017,** *72*, 130-147.

15. Li, L.; Jiang, S.; Li, X.; Liu, Y.; Su, J.; Chen, J., Recent advances in trimethoxyphenyl (TMP) based tubulin inhibitors targeting the colchicine binding site. *Eur. J. Med. Chem.* **2018,** *151*, 482-494.

16. Yee, K. W.; Hagey, A.; Verstovsek, S.; Cortes, J.; Garcia-Manero, G.; O'Brien, S. M.; Faderl, S.; Thomas, D.; Wierda, W.; Kornblau, S.; Ferrajoli, A.; Albitar, M.; McKeegan, E.; Grimm, D. R.; Mueller, T.; Holley-Shanks, R. R.; Sahelijo, L.; Gordon, G. B.; Kantarjian, H. M.; Giles, F. J., Phase 1 study of ABT-751, a novel microtubule inhibitor, in patients with refractory hematologic malignancies. *Clin. Cancer Res.* **2005,** *11* (18), 6615-6624.

17. Rudin, C. M.; Mauer, A.; Smakal, M.; Juergens, R.; Spelda, S.; Wertheim, M.; Coates, A.; McKeegan, E.; Ansell, P.; Zhou, X.; Qian, J.; Pradhan, R.; Dowell, B.; Krivoshik, A.; Gordon, G., Phase I/II study of pemetrexed with or without ABT-751 in advanced or metastatic non-small-cell lung cancer. *J. Clin. Oncol.* **2011,** *29* (8), 1075-1082.

18. Mauer, A. M.; Cohen, E. E.; Ma, P. C.; Kozloff, M. F.; Schwartzberg, L.; Coates, A. I.; Qian, J.; Hagey, A. E.; Gordon, G. B., A phase II study of ABT-751 in patients with advanced non-small cell lung cancer. *J. Thorac. Oncol.* **2008,** *3* (6), 631-636.

19. Zheng, S.; Zhong, Q.; Mottamal, M.; Zhang, Q.; Zhang, C.; LeMelle, E.; McFerrin, H.; Wang, G., Design, Synthesis, and Biological Evaluation of Novel Pyridine-Bridged Analogues of Combretastatin-A4 as Anticancer Agents. *J. Med. Chem.* **2014,** *57* (8), 3369-3381.

20. Zhou, Z. -Z.; Shi, X. -D.; Feng, H. -F.; Cheng, Y. -F.; Wang, H.-T.; Xu, J.-P., Discovery of 9H-purins as potential tubulin polymerization inhibitors: Synthesis, biological evaluation and structure−activity relationships. *Eur. J. Med. Chem.* **2017,** *138*, 1126-1134.

21. Ge, B. -C.; Feng, H.-F.; Cheng, Y.-F.; Wang, H.-T.; Xi, B.-M.; Yang, X.-M.; Xu, J.-P.; Zhou, Z.-Z., Design, synthesis and biological evaluation of substituted aminopyridazin-3(2H)-ones as G0/G1-phase arresting agents with apoptosis-inducing activities. *Eur. J. Med. Chem.* **2017,** *141* (Supplement C), 440-445.

22. Yan, G.-H.; Li, X.-F.; Ge, B.-C.; Shi, X.-D.; Chen, Y.-F.; Yang, X.-M.; Xu, J.-P.; Liu, S.-W.; Zhao, P.-L.; Zhou, Z.-Z.; Zhou, C.-Q.; Chen, W.-H., Synthesis and anticancer activities of 3-arylflavone-8-acetic acid derivatives. *Eur. J. Med. Chem.* **2015,** *90* (0), 251-257.

23. Torres, F. C.; Garcia-Rubino, M. E.; Lozano-Lopez, C.; Kawano, D. F.; Eifler-Lima, V. L.; von Poser, G. L.; Campos, J. M., Imidazoles and Benzimidazoles as Tubulin-Modulators for Anti-Cancer Therapy. *Curr. Med. Chem.* **2015,** *22* (11), 1312-1323.

24. Ashraf, M.; Shaik, T. B.; Malik, M. S.; Syed, R.; Mallipeddi, P. L.; Vardhan, M. V. P. S. V.; Kamal, A., Design and synthesis of cis-restricted benzimidazole and benzothiazole mimics of combretastatin A-4 as antimitotic agents with apoptosis inducing ability. *Bioorg. Med. Chem. Lett.* **2016,** *26* (18), 4527-4535.

25. Fu, D.-J.; Yang, J.-J.; Li, P.; Hou, Y.-H.; Huang, S.-N.; Tippin, M. A.; Pham, V.; Song, L.; Zi, X.; Xue, W.-L.; Zhang, L.-R.; Zhang, S.-Y., Bioactive heterocycles containing a 3,4,5-trimethoxyphenyl fragment exerting potent antiproliferative activity through microtubule destabilization. *Eur. J. Med. Chem.* **2018,** *157*, 50-61.

26. Kamal, A.; Rao, A. V. S.; Nayak, V. L.; Reddy, N. V. S.; Swapna, K.; Ramakrishna, G.; Alvala, M., Synthesis and biological

evaluation of imidazo[1,5-a]pyridine-benzimidazole hybrids as inhibitors of both tubulin polymerization and PI3K/Akt pathway. *Org. Biomol. Chem.* **2014,** *12* (48), 9864-9880.

27. Kamal, A.; Shaik, A. B.; Polepalli, S.; Kumar, G. B.; Reddy, V. S.; Mahesh, R.; Garimella, S.; Jain, N., Synthesis of arylpyrazole linked benzimidazole conjugates as potential microtubule disruptors. *Bioorg. Med. Chem.* **2015,** *23* (5), 1082-1095.

28. Gaspari, R.; Prota, A. E.; Bargsten, K.; Cavalli, A.; Steinmetz, M. O., Structural Basis of cis- and trans-Combretastatin Binding to Tubulin. *Chem* **2017,** *2* (1), 102-113.

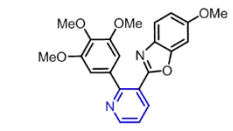

29

Anti-tubulin IC_{50} = 2.1 μM
Cell proliferation GI_{50} = 0.27 ~ 2.1 μM

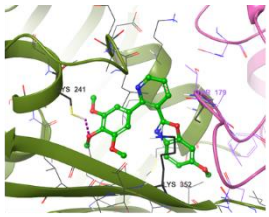

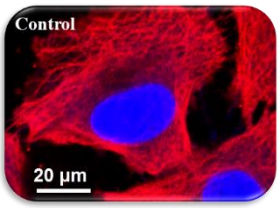

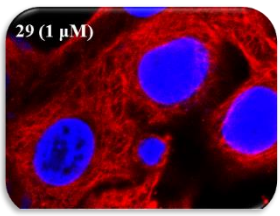

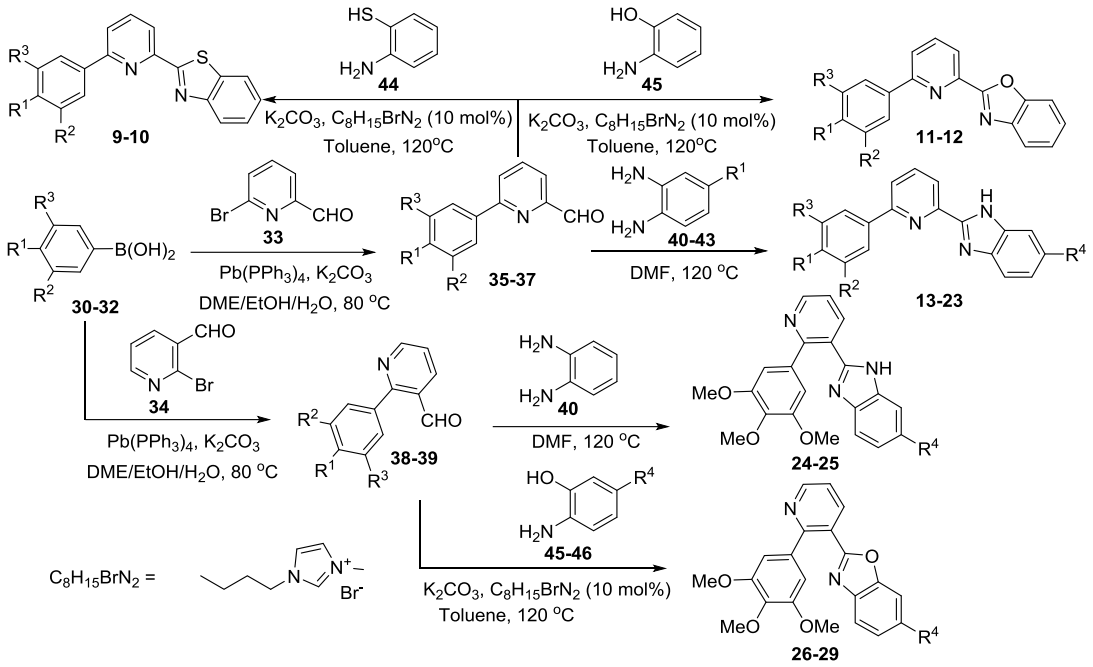
9-10
44
45
K2CO3, C8H15BrN2 (10 mol%)
Toluene, 120°C
K2CO3, C8H15BrN2 (10 mol%)
Toluene, 120°C
11-12
30-32
33
Pb(PPh3)4, K2CO3
DME/EtOH/H2O, 80 °C
35-37
40-43
DMF, 120 °C
13-23
34
Pb(PPh3)4, K2CO3
DME/EtOH/H2O, 80 °C
38-39
40
DMF, 120 °C
24-25
45-46
K2CO3, C8H15BrN2 (10 mol%)
Toluene, 120 °C
26-29
C8H15BrN2 =

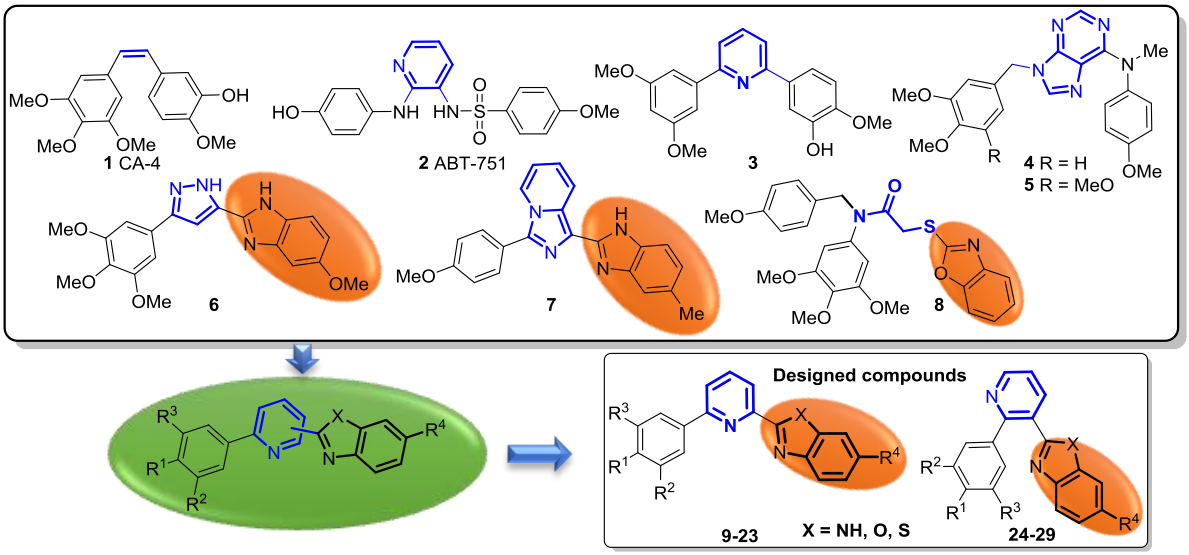
1 CA-4
2 ABT-751
3
4 R = H
5 R = MeO
6
7
8
Designed compounds
9-23
X = NH, O, S
24-29

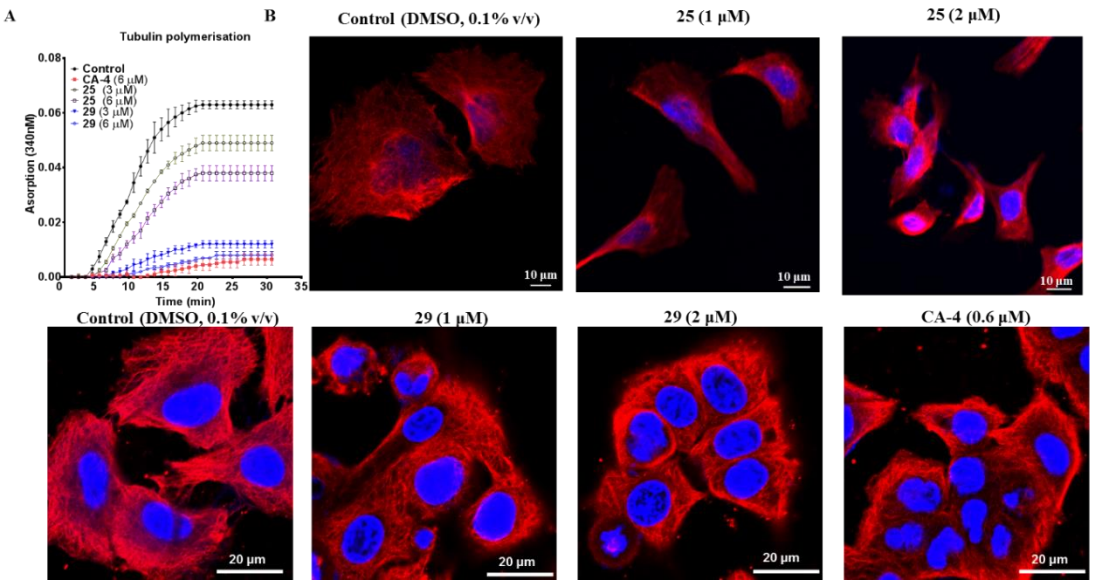
A
B
Tubulin polymerisation
Control
CA-4 (6 μM)
25 (3 μM)
25 (6 μM)
29 (3 μM)
29 (6 μM)
Asorption (340nM)
Time (min)
Control (DMSO, 0.1% v/v)
25 (1 μM)
25 (2 μM)
Control (DMSO, 0.1% v/v)
29 (1 μM)
29 (2 μM)
CA-4 (0.6 μM)
10 μm
20 μm

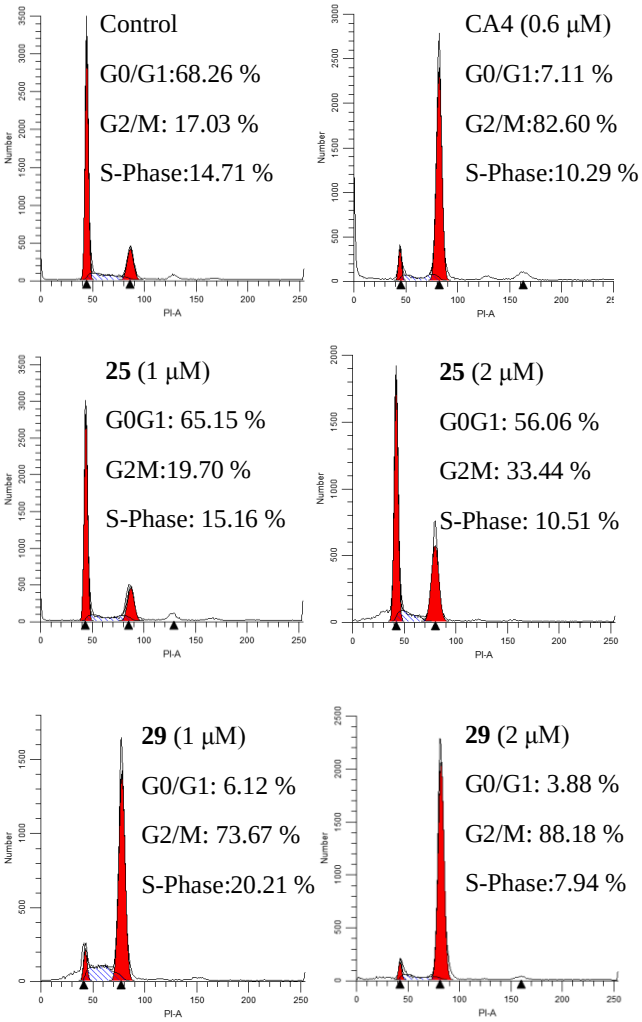
Control
G0/G1:68.26 %
G2/M: 17.03 %
S-Phase:14.71 %
CA4 (0.6 µM)
G0/G1:7.11 %
G2/M:82.60 %
S-Phase:10.29 %
25 (1 µM)
G0G1: 65.15 %
G2M:19.70 %
S-Phase: 15.16 %
25 (2 µM)
G0G1: 56.06 %
G2M: 33.44 %
S-Phase: 10.51 %
29 (1 µM)
G0/G1: 6.12 %
G2/M: 73.67 %
S-Phase:20.21 %
29 (2 µM)
G0/G1: 3.88 %
G2/M: 88.18 %
S-Phase:7.94 %
Number
PI-A

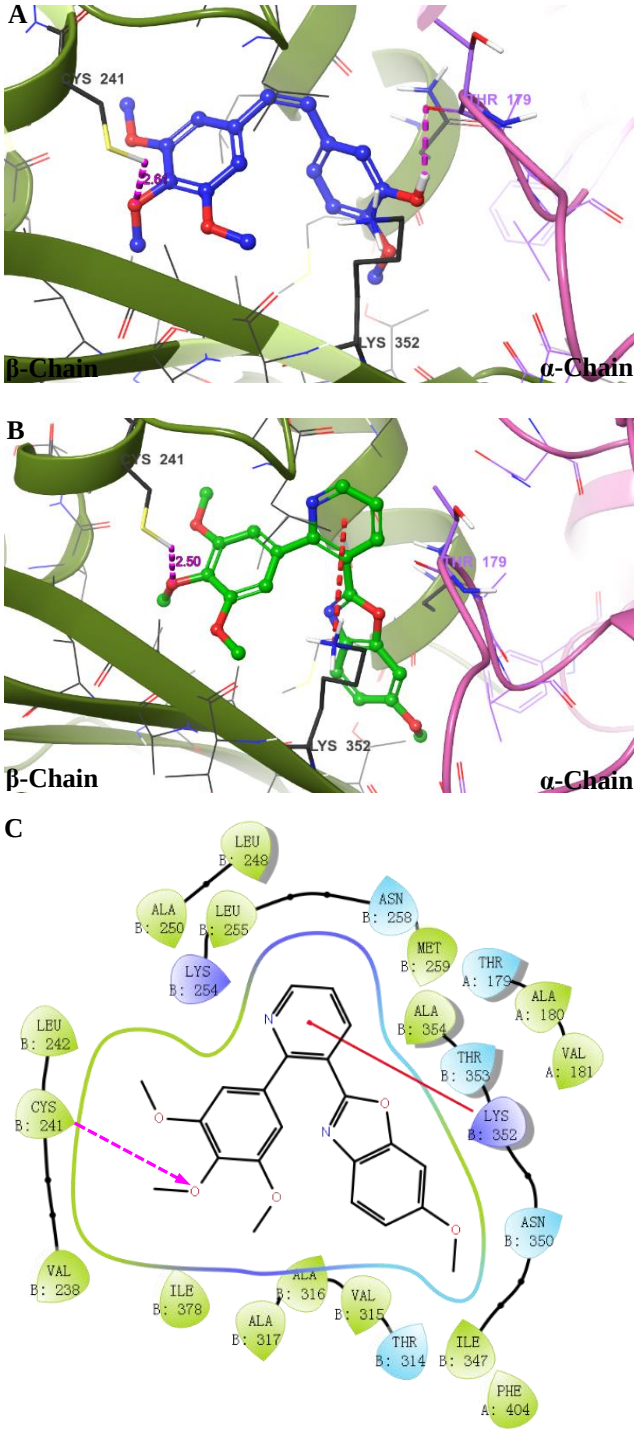
A
CYS 241
THR 179
2.64
LYS 352
β-Chain
α-Chain
B
CYS 241
2.50
THR 179
LYS 352
β-Chain
α-Chain
C
LEU B: 248
ALA B: 250
LEU B: 255
ASN B: 258
MET B: 259
THR A: 179
ALA A: 180
LYS B: 254
ALA B: 354
VAL A: 181
LEU B: 242
THR B: 353
CYS B: 241
LYS B: 352
ASN B: 350
VAL B: 238
ILE B: 378
ALA B: 316
VAL B: 315
ALA B: 317
THR B: 314
ILE B: 347
PHE A: 404

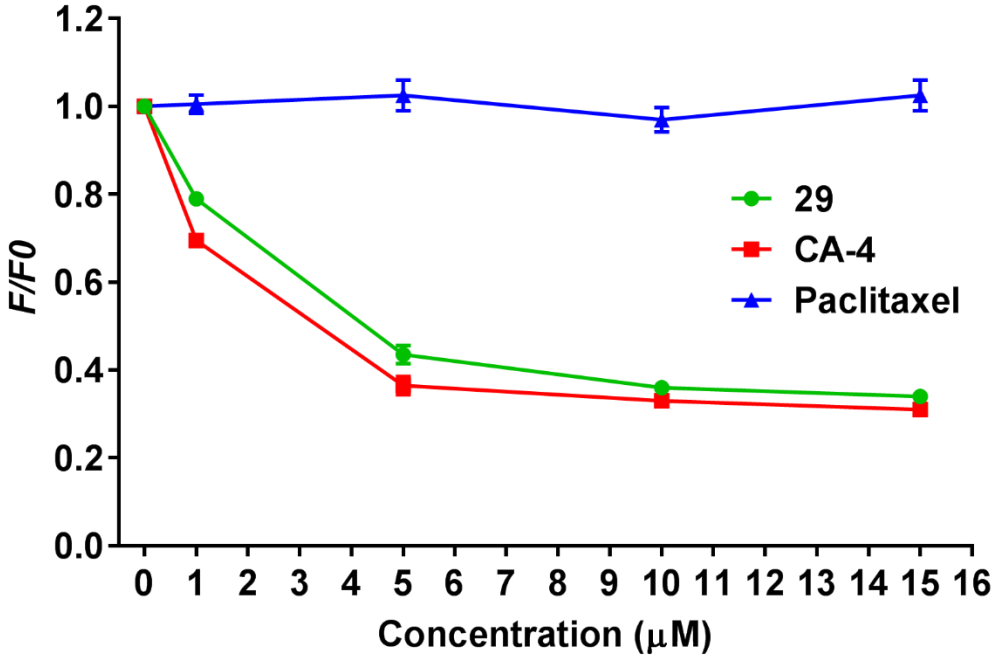
1.2
1.0
0.8
0.6
0.4
0.2
0.0
F/F0
0 1 2 3 4 5 6 7 8 9 10 11 12 13 14 15 16
Concentration (μM)
29
CA-4
Paclitaxel